

Available online at [www.sciencedirect.com](http://www.sciencedirect.com)

ScienceDirect

journal homepage: [www.elsevier.com/locate/oceano](http://www.elsevier.com/locate/oceano)

ORIGINAL RESEARCH ARTICLE

# Thermoelastic surface properties of seawater in coastal areas of the Baltic Sea

Katarzyna Boniewicz-Szmyt<sup>a,\*</sup>, Stanisław J. Pogorzelski<sup>b</sup><sup>a</sup> Department of Physics, Gdynia Maritime University, Gdynia, Poland<sup>b</sup> Institute of Experimental Physics, University of Gdańsk, Gdańsk, Poland

Received 13 August 2015; accepted 17 August 2015

Available online 3 September 2015

## KEYWORDS

Baltic Sea;  
Surface tension;  
Crude oil-seawater interface;  
Thermodynamic parameters;  
Surface viscoelasticity

**Summary** Correlations and data for the thermoelastic surface properties of seawater were determined by means of surface tension-temperature and surface pressure-area isotherm measurements performed in Baltic Sea coastal waters (Gulf of Gdańsk, Poland). Thermodynamic surface parameters examined include: surface free energy- $\gamma$ , entropy, enthalpy, surface specific heat of air-seawater (AW), air-crude oil (AO) and crude oil-seawater (OW) interfaces, and the surface elasticity was quantified in terms of complex viscoelasticity modules with relaxation times of the transition processes. The spatial and temporal evolution of the parameters differed significantly from the literature data for seawater since the effect of surface active substances of natural and municipal origin was likely to be present in these coastal waters. The seawater surface turned out to have the viscoelastic 2D character as well as other interfacial systems AO and OW where three crude oils in contact with the seawater were studied for comparison. The dilational elasticity modules were found to follow the sequence  $E_{AW} > E_{OW} > E_{AO}$ . Composite oil lens-covered seawater exhibited a significant drop of  $E$  from  $E_{AW}$  (crude oil free surface) even for low oil coverage fraction  $F_0$ .

The obtained surface and interfacial tension-temperature dependences allowed to correct the spreading coefficient ( $S = \gamma_{AW} - \gamma_{AO} - \gamma_{OW}$ ) to the desired temperature range, for example. The latter parameter with the sea surface elasticity data allows one to test the modified model of crude oil spreading proposed by the authors (Boniewicz-Szmyt and Pogorzelski, 2008), for spreading kinetics phenomenon at the surface-tension regime.

© 2015 Institute of Oceanology of the Polish Academy of Sciences. Production and hosting by Elsevier Sp. z o.o. This is an open access article under the CC BY-NC-ND license (<http://creativecommons.org/licenses/by-nc-nd/4.0/>).

\* Corresponding author at: Department of Physics, Gdynia Maritime University, Morska 81-87, 81-225 Gdynia, Poland. Tel.: +48 585232250. E-mail addresses: [kbon@am.gdynia.pl](mailto:kbon@am.gdynia.pl) (K. Boniewicz-Szmyt), [fizsp@ug.edu.pl](mailto:fizsp@ug.edu.pl) (S.J. Pogorzelski).  
Peer review under the responsibility of Institute of Oceanology of the Polish Academy of Sciences.



Production and hosting by Elsevier

<http://dx.doi.org/10.1016/j.oceano.2015.08.003>

0078-3234/© 2015 Institute of Oceanology of the Polish Academy of Sciences. Production and hosting by Elsevier Sp. z o.o. This is an open access article under the CC BY-NC-ND license (<http://creativecommons.org/licenses/by-nc-nd/4.0/>).

## 1. Introduction

The knowledge of seawater surface thermal and elastic properties is important in several surface tension-mediated processes like: wind waves generation and damping, gas bubbles formation, sea foam and oil emulsion stability, spreading and kinetics of contamination expansion, for instance. Literatures contain many data for the properties of seawater, but only a few sources provide full coverage for all of these properties. The data are mainly based on experimental measurements carried out in and before the 1970s, and usually span a limited temperature and salinity range. Most of the data require interpolation and extrapolation to conditions of interest, and not all desirable properties are given, particularly transport and surface elastic properties affecting to a great extent physical and dynamical oceanographical processes mediated by interfaces. The International Association for the Properties of Steam (IAPS) has approved an international table of values for the surface tension (ST) of water in equilibrium with its vapor over the entire liquid range (Vargaftik et al., 1983). However, seawater is a particular water phase which SF can significantly differ from the recent reference dependences (Sharqawy et al., 2010), particularly in coastal waters enriched in surface-active contaminants (Pogorzelski and Kogut, 2003). As a first approximation, most physical properties of seawater are similar to those of pure water, which can be described by functions of temperature. The general trend for liquid surface tension is that it decreases with an increase of temperature. Solutes can have different effects on surface tension depending on their structure. Inorganic salts, which are the type of salts in seawater, increase the surface tension of the solution. Organic contamination in seawater may also have a considerable effect on the surface tension, particularly when surfactants, capable of forming surface layers of surface elasticity  $E$ , are involved. Any relative area change  $\Delta A/A$  of the interfacial system of dilational elasticity modulus  $E$  leads to the surface tension drop from the initial value  $\gamma_{AW}$  to  $\gamma_{AW} - E(\Delta A/A)$ , as demonstrated in Boniewicz-Szmyt and Pogorzelski (2008), where kinetics model of crude oil spreading at sea was corrected. Since the spreading phenomenon depends on the spreading coefficient  $S = \gamma_{AW} - \gamma_{AO} - \gamma_{OW}$ , the remaining interfacial tensions A/O, O/W and their temperature dependences, for the exemplary crude oils in contact with seawater, were evaluated during the course of this study. Moreover, the commonly met at sea composite surface consisting of lens-shaped crude oil areas covering a fraction  $F_0$  was also considered.

A certain fraction of dissolved organic matter (DOM) in the sea has surface-active (SA) properties and makes up a very reactive part of the organic matter (Druffel and Bauer, 2000). According to their SA properties, these substances accumulate at marine interfaces thereby influencing gas, mass, momentum and energy transfer between the thus modified interfaces. The composition of sea surface films is largely undefined, although significant enrichments of many specific classes of compounds in the surface microlayer have been demonstrated (for review, see Hunter and Liss, 1981). Natural sea films most resemble layers composed of proteins, polysaccharides, humic-type materials and long chain aliphatic acid esters (Van Vleet and Williams, 1983). In particular, the Polish coastal zone of the southern Baltic Sea is a

recipient of riverine waters and remains under severe anthropogenic pressure that leads to formation films of undefined composition with a complex interfacial architecture. The exhibited natural film parameters variability with the environmental factors (film temperature, ionic strength, pH of the aqueous subphase, wind speed, time scale of relaxation processes taking place in a multicomponent natural film) have been already discussed in detail elsewhere (Mazurek et al., 2008).

The aim of the paper was twofold: (1) to determine the apparent sea surface thermodynamic functions (entropy, enthalpy, surface tension, surface specific heat), and their temperature variability also in the contact with model crude oils; (2) to quantify the surface-active substances effect on the dilational viscoelasticity of the seawater surface in shallow coastal areas of the Baltic Sea and on the interfacial systems: crude oil/seawater and air/crude oil affecting composite air/crude oil/seawater surface elasticity. The collected data will be further used in the corrected model of crude oil spreading at sea proposed by the authors (Boniewicz-Szmyt and Pogorzelski, 2008), for model evaluations.

## 2. Surface thermodynamics and viscoelasticity – theory

### 2.1. Thermodynamic functions

In the studies of ST of liquids, one needs data for calibration of instruments at different temperatures. The variation of  $\gamma$  for water with temperature  $t$  [°C] is given as follows by various investigators, as reviewed in Vargaftik et al. (1983).

By Harkins (1952):

$$\gamma_{\text{water}} = 75.680 - 0.138t - 0.05356t^2 + 0.0647t^3. \quad (1)$$

The high accuracy is important in such data, since we use these for calibration purposes. More recent and reliable data by Cini et al. (1972) indicate that

$$\gamma_{\text{water}} = 75.668 - 0.139t - 0.2885 \times 10^{-3}t^2. \quad (2)$$

The International Association for the Properties of Steam (IAPS) has approved an international table of values for the surface tension of water in equilibrium with its vapor over the entire liquid range (Vargaftik et al., 1983). However, seawater is a particular water phase which SF can differ significantly from the recent reference dependences (Sharqawy et al., 2010), particularly in coastal waters enriched in surface-active contaminants and solid dust particles (Pogorzelski and Kogut, 2003). The surface entropy and total enthalpy (per unit area) can be derived from ST versus  $T$  dependence (Adamson and Gast, 1997).

The surface entropy,  $S_s$ , corresponding to the above relation is

$$S_s = \frac{-d\gamma}{dT} \quad (3)$$

and the corresponding expression for surface enthalpy,  $H_s$ , is

$$H_s = \gamma - T \left( \frac{d\gamma}{dT} \right). \quad (4)$$

Since ST is a type of Helmholtz free energy, the expression for surface entropy is  $S_s = -d\gamma/dT$ . Hence, an amount of heat ( $H_s$ )

must be generated and absorbed by the liquid when the surface is extended.

The surface specific heat  $C_s$  is given as:

$$C_s = \frac{dH_s}{dT}. \quad (5)$$

Since  $d\gamma/dT$  is negative equal to  $-0.16 \text{ mN m}^{-1} \text{ K}^{-1}$  (for pure water),  $H_s$  is greater than  $\gamma$ . The entropic term in Eq. (4) takes into account the energy losses related to the new surface creation.  $H_s$  is frequently the more informative of the two quantities, or at least it is more easily related to molecular arrangements at the interface.

## 2.2. Viscoelasticity modules – effect of surfactants and solid particles

Elastic surfactant film parameters may be derived from the surface pressure-film area  $(\pi-A)_T$  isotherm and the surface pressure-temperature  $(\pi-T)_A$  isochore. A drop of the surface tension, i.e. the surface film pressure  $\pi = \gamma_0 - \gamma$ , where  $\gamma_0$  and  $\gamma$  are the surface tension of solvent (water) and seawater surfactant solution, respectively. Consequently,  $d\gamma = -d\pi$ .

The simplest equation of state to describe surface films is the 2D analog of the ideal gas law (Adamson and Gast, 1997):

$$\pi A_m = kT, \quad (6)$$

where  $k$  is the Boltzmann constant,  $A_m$  the area per film molecule related to the Gibb's adsorption  $\Gamma$ ,  $A_m = 1/\Gamma N_A$ ,  $N_A$  – the Avogadro number and  $T$  is the temperature in Kelvin. The description of the 2D film states depends on the dilational elasticity modulus (or Gibb's modulus)  $E_{isoth}$  expressing the static, compressional response of a film to compression or dilation corresponding to the isotherm registration in its thermodynamic equilibrium:

$$E_{isoth} = -A \left( \frac{d\pi}{dA} \right)_T. \quad (7)$$

The establishment of the thermodynamic equilibrium in the film is not trivial. The effect depends on the dimensionless parameter Deborah number ( $De$ ) defined as the ratio of the film relaxation time  $\tau$  to the "time of observation" (a reciprocal of the strain rate of a film:  $t_{obs} = [(dA/A)/dt]^{-1}$ ), as argued in Kato et al. (1992). The interfacial system appears to be at the quasi-equilibrium thermodynamic state if  $De$  number is less than unity. Any relaxation process in films leads to dilational viscoelasticity, and the surface dilational viscoelastic modulus  $E$  is a complex quantity composed of real  $E_d$  (dilational elasticity) and imaginary  $E_i$  ( $=\omega\eta_d$ , where  $\eta_d$  is the dilational viscosity) parts  $E = E_d + iE_i = E_0 \cos \varphi + iE_0 \sin \varphi$ , where  $\omega$  is the angular frequency of periodic area oscillations,  $E_0 = -\Delta\pi/(\Delta A/A)$  represents the amplitude ratio between the surface stress and strain, and  $\varphi$  is the loss angle of the modulus (Ravera et al., 2005). For surface layers exhibiting a pure elastic behavior, the linear relation between  $\Delta\pi$  and  $\Delta A$  appears, as shown by Eq. (7). In the case of the viscoelastic film, the relation contains an additional term depending on the surface deformation rate:

$$\Delta\pi = E_{isoth} \cdot \Delta A/A + \eta_d d(\Delta A/A)/dt. \quad (8)$$

Diffusional relaxation time  $t_r$  is fully described by SA properties of the substance forming the monolayer (Joos and Bleys, 1983):

$$t_r = \left[ a/\Gamma_\infty (1 + c/a)^2 \sqrt{D} \right]^{-2}, \quad (9)$$

where  $a$  is the Szyszkowski's surface activity coefficient,  $\Gamma_\infty$  the saturation adsorption,  $c$  the molar concentration of a surfactant, and  $D$  is the diffusion coefficient.

For more complex structurally surface films, the time scale of the molecular relaxation processes taking place in surface films, and the viscoelasticity modulus parts can be experimentally derived from the stress-relaxation studies (Van Hunsel and Joos, 1989).

The surface pressure-time  $(\pi-t)$  response of a film to a rapid step ( $\Delta t = 0.2-1.5$  s) relative surface area deformation  $\Delta A/A_0$  ( $=0.07-0.23$ ) is registered, and presented in the following form (Nino et al., 1998):

$$\ln \frac{\pi_\infty - \pi_t}{\pi_\infty - \pi_0} = -\lambda_1 t, \quad (10)$$

where  $\pi_\infty$ ,  $\pi_0$ , and  $\pi_t$  are the surface pressures at steady-state condition ( $t \rightarrow \infty$ ), at time  $t = 0$ , and at any time  $t$ ;  $\lambda_1$  is the first-order rate constant related to the relaxation time  $\tau_1$  ( $=1/\lambda_1$ ).

In the framework of a model for dilational visco-elasticity, adapted to the stepwise  $\rightarrow$  surface  $\rightarrow$  area;  $\rightarrow$  deformation mode, the real and imaginary parts of  $E$  can be obtained from the following relations (Aksenenko et al., 2006; Jayalakshmi et al., 1995):

$$E_d = E_0 \left[ \frac{(1 + \Omega)}{(1 + 2\Omega + 2\Omega^2)} \right] \quad \text{and} \quad E_i = E_0 \left[ \frac{\Omega}{(1 + 2\Omega + 2\Omega^2)} \right], \quad (11)$$

$$E_0 = \frac{(\pi_0 - \pi_\infty)}{(\Delta A/A_0)} \quad \text{is an amplitude of the modulus } E, \quad (12)$$

where

$$\Omega = \sqrt{\frac{\Delta t}{\tau_1}} \quad \text{and} \quad \text{tg}\varphi = \frac{\Omega}{1 + \Omega}, \quad (13)$$

$$|E| = \sqrt{E_d^2 + E_i^2} \quad \text{is the modulus of the complex quantity } E, \quad (14)$$

and  $\Delta t$  is the applied step film area deformation time.

At sufficiently low film area compression rates ( $De \ll 1$ ), the dilational viscoelasticity modulus can be approximated by  $E_{isoth}$ . Keeping in mind that dry dust loads can be trapped at the sea water interface, the mineral particles effect on  $E$  should be addressed.

Considering the total surface covered with a collection of the solid spherical particles of  $R$  radius at the surface concentration  $n$  (particles per unit area), and remaining particle-free liquid surface (having  $E_{free}$  modulus), for the modulus of the composite surface  $E_{com}$  we have (Lucassen, 1992):

$$E_{com} = \frac{E_{free}}{\left\{ 1 + n\pi R^2 \left[ (2E_{free} \cos^2 \theta / \gamma_{LV}) - \sin^2 \theta \right] \right\}}. \quad (15)$$

A position of a solid spherical particle at the air/water interface depends on the hydrophilic (particle material/water contact angle  $\theta < 90^\circ$ ) and hydrophobic ( $CA > 90^\circ$ ) character of the spherical particles. A solid particle which is spherical and so small (in reference to the capillary length, i.e.  $R \ll (2\gamma_{LV}/\rho_L g)^{1/2}$ , where  $\gamma_{LV}$  and  $\rho_L$  are the surface tension and density of the liquid phase, respectively) that gravity can be ignored if compared to the surface forces, will adopt a position in the air-fluid interface which is fully determined by the wetting angle (Adamson and Gast, 1997).

As can be noticed, the presence of partially wetted spherical particles can either increase or decrease the apparent dilational modulus of the whole surface depending on the sign of the term within brackets in the denominator of Eq. (15). Thus, when  $\theta$  is close to  $90^\circ$ , or when  $E_{free}/\gamma_{LV}$  (values  $\sim 0.1$  are found in practice) is very small, there will be increase. In contrast, when  $\theta$  is close to  $0^\circ$  or when  $E_{free}/\gamma_{LV}$  is large, the surface dilational modulus will decrease due to the presence of particles.

Environmental dust characteristics (particle size distribution, wettability of dust material, and surface deposition flux) in Baltic Sea coastal waters and their effect on sea surface viscoelasticity are reported in the accompanying paper (Boniewicz-Szmyt and Pogorzelski, 2015).

### 3. Experimental methodology

#### 3.1. Sampling sites

Natural marine surfactant film surface rheology and adsorption studies in shallow off-shore waters of the Baltic Sea (Gulf of Gdańsk, Poland) were carried out in the period from November 2012 to November 2013 at selected locations along the coast from Brzeźno to Gdynia. Sea surface microlayer samples were collected mostly under calm sea conditions ( $V_{10} < 4 \text{ m s}^{-1}$ ;  $V_{10}$  is the wind speed at the standard height = 10 m).

#### 3.2. Natural film rheology – methods

The novel film sampler is a submersible rectangular double-walled vessel, integrated with the Langmuir trough, which “cuts out” an undisturbed sea area region measuring  $45 \text{ cm} \times 35 \text{ cm}$  and 8 cm thick. The most valuable property of this device is that the collection and Langmuir trough isotherm and isochore analyses are performed without transferring and any chemical processing of the microlayer material, as described in detail elsewhere (Pogorzelski, 1992; Pogorzelski et al., 1994). The film analyses were performed immediately after sampling. Underlying water was collected by immersing a 1 L glass bottle at a depth of 0.5–1.5 m. To perform surface isotherm studies, the initial Langmuir trough area  $A_0 = 1,200 \text{ cm}^2$  is compressed with an average deformation speed  $v = 0.6 \text{ cm}^2 \text{ s}^{-1}$  (corresponding to  $De$  value  $\sim 0.09$ ) by moving two PTFE-coated glass sliders toward each other symmetrically around the film pressure sensor. Surface tension was measured with a Wilhelmy plate technique using a piece of filter paper (5 cm wide) attached to the arm of a electrobalance (GM2 + UL5, Scaime, France). They were accurate to within  $0.1 \text{ mN m}^{-1}$ . Dynamic film characteristics were evaluated from stress-relaxation studies (Van Hunsel and Joos, 1989). The surface pressure-time response  $\pi(t)$  of a

film to a rapid ( $\Delta t = 0.19\text{--}1.1 \text{ s}$ ) relative surface area deformation  $\Delta A/A_0 (=0.07\text{--}0.23)$  applied to the sample by barrier movement was registered for several minutes. The reported static, dynamic and thermodynamic surface parameters stand for an average value over 6–9 measuring runs performed at the given site. The sampler, leveling device, electrobalance sensor resting on the measuring table were situated near the sampling site on the shore (see Fig. 1). Surface tension was measured in the temperature range 3–14°C for seawater samples heated from the Langmuir trough bottom realized with a water thermostated system (temperature controlled with accuracy  $0.1^\circ\text{C}$  using a thermocouple). A detailed description of the measuring procedures and physical conditions adopted in surface pressure-area isotherm and dynamic surface pressure registrations can be found in Pogorzelski et al. (2006). For in situ seawater surfactants adsorption dynamics studies a hand-held bubble pressure tensiometer (BP 2100 PocketDyne, Krüss, Germany) with the adjustable bubble surface formation age was used.

A new type of Langmuir trough has been used for force-area and stress-relaxation studies, for A/O and O/W interfaces. Fig. 2 illustrates the essential features of the apparatus. A solid PTFE frame, or barrier, sits in a rectangular PTFE trough of dimensions  $90 \text{ cm} \times 60 \text{ cm} \times 6 \text{ cm}$ . The barrier has four, rigid solid sides 60 cm long and 5 cm high. The barrier contains the film of interest, which is omni-directionally expanded or compressed by flexing the corners, so changing the shape of the barrier. The four sides are hinged at the corners so that they provide a continuous, leak-free enclosure. The walls have PTFE pegs underneath so that liquid (generally the aqueous phase) can flow under the walls to create a well defined interfacial area inside the barrier. Two opposite corners of the barrier are connected to a geared stepper motor. The rhomboidal shape change on driving together the two opposite corners of the trough produces the area change  $A_r$  from 3,600 to 600  $\text{cm}^2$ . The interfacial tension/pressure is measured with a Wilhelmy plate dipping into the interface, at the center of the film, suspended from a force transducer (GM2 + UL5, Scaime, France).

For measurements at an O/W interface a 6–7 mm layer of oil is gently layered over the top of the aqueous phase. A

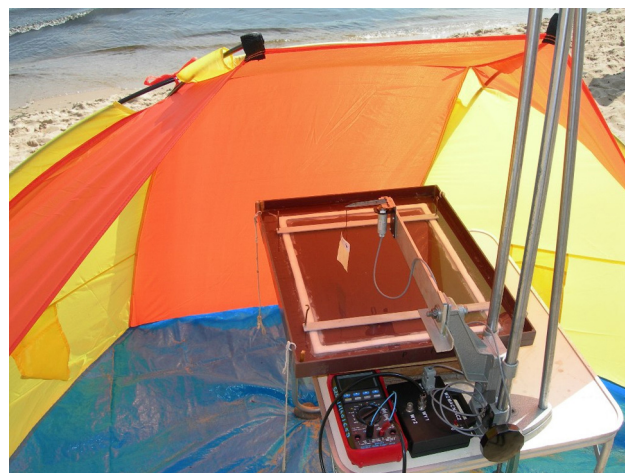


**Figure 1** Experimental set-up for at-field natural sea surface film studies located near-by the southern shore line of the Baltic Sea (Jelitkowo, Gulf of Gdańsk).



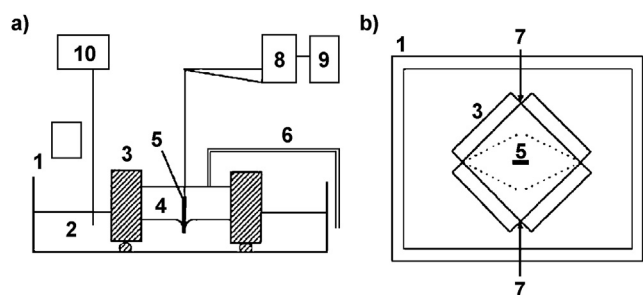


**Figure 2** Schematic illustration of the frame-shaped Langmuir trough apparatus, for O/W interface studies: view from side (a) and above (b). Denotations: 1 – trough walls, 2 – lower (aqueous phase), 3 – frame-barrier, 4 – upper (oil phase), 5 – hydrophobic Wilhelmy plate, 6 – siphon (peristaltic pump system), 7 – direction of stepper motor drive for film compression, 8 – force transducer, 9 – multimeter. Area change: initial (solid line) → final (dotted line).

hydrophobic plate is completely submerged beneath the surface of the oil layer and suspended at the O/W interface by two thin stainless steel wires. On compression/expansion, the oil volume and the O/W interface are completely contained within the barrier. A change in the height of the interface causes a slight change in the buoyant force on the Wilhelmy plate. This complication is avoided by maintaining the height of the oil level constant by a siphon system. As a film is compressed the surface of the oil is continually sucked off via a peristaltic pump, to maintain a constant level (on expansion the oil can be pumped back). The film may be compressed at constant slow speed (used for  $\pi$ -A isotherms), or be subjected to a sudden rapid compression and the resultant  $\pi$  versus time  $t$  decay plot monitored.

## 4. Results and discussion

### 4.1. Surface thermodynamic parameters

An exemplary surface tension  $\gamma_{AW}$  versus temperature dependence registered at Brzeźno on 31 January 2013, is shown in Fig. 3, where reference data (Eq. (2) and Eq. (25)) from Sharqawy et al. (2010), for pure distilled and artificial seawater of 6 PSU salinity, respectively, are also included. In general, a linear plot is observed ( $R^2 \approx 1$ ). The experimental dependences of practical value, provided for all the studied sites, allow one to correct the surface thermodynamic data to the desired temperature. Values of  $S_s$  for reference water surfaces are almost the same as well as the particular  $\gamma_{AW}$  values for the given temperature in the range of interest (2–16°C). Both  $S_s$  and  $\gamma_{AW}$  took higher values for Baltic Sea water sample.

Higher values of  $S_s$  point to the less complex interfacial layer structure consisting of adsorbed surface active substances and counter ions present in the sub-layer water phase. The double electric layer likely to be found here creates an interfacial system of particular thermodynamics (of higher work of cohesion =  $W_{coh} = 2\gamma_{AW}$ ; Butt et al., 2003). For instance, the surface active substance (SAS) adsorption leads to the surface tension drop  $d\gamma = -\Gamma d\mu$ , where  $\mu$  is the chemical potential, and the Gibbs surface excess  $\Gamma = d\gamma/RT$ , for a gaseous surface film (Adamson and Gast, 1997).

Surface free energy  $\gamma_{AW}$  and surface enthalpy versus temperature dependences are shown in Fig. 4, for Baltic Sea water sample collected at Gdynia-Orłowo on 17 April 2013. A linear plot versus  $T$  can be approximated with a relation  $\gamma_{AW} = -0.149T + 77.696$ .  $H_s$  was almost a constant only slightly leveling down as  $T$  increased which lead to rather low surface specific heat  $C_s$  values.

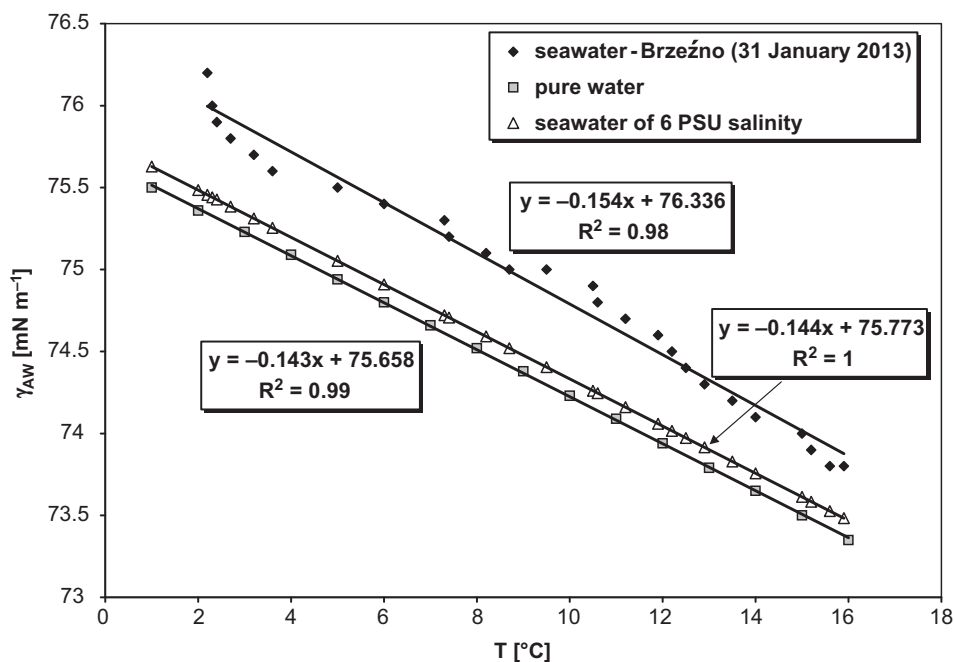


**Figure 3** Seawater surface tension  $\gamma_{AW}$  versus temperature, for Baltic Sea sample collected at Brzeźno on 31 January 2013. The reference relations (Eq. (2) and Eq. (25)) from Sharqawy et al. (2010) are included, for pure distilled water and seawater of 6 PSU salinity, respectively.

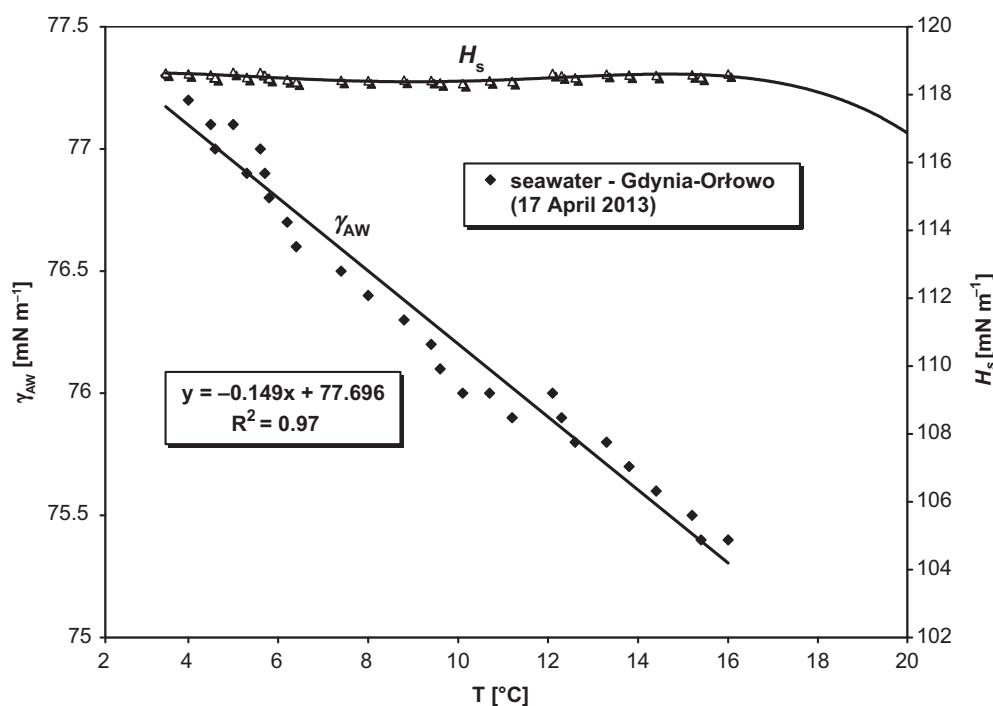


**Figure 4** Surface free energy  $\gamma_{AW}$  and enthalpy versus  $T$ , for Baltic Sea water sample collected at Gdynia-Orłowo on 17 April 2013.

Such dependences measured at a few sampling stations allowed estimation of the surface thermodynamics functions collected in Table 1.

The parameters were corrected to the long-term surface temperature of the Baltic Sea ( $= 7.66^\circ\text{C}$ ). As a reference, surface tension seawater characteristics (derived from Eq. (25) from Sharqawy et al. (2010), for 6 PSU salinity characteristic) for the studied area were taken.

Surface tension of original Baltic Sea water samples was higher by 1.21–2.71  $\text{mN m}^{-1}$  in reference to the salty (6 PSU) but also surfactant-free seawater. In solutions of inorganic salts the surface tension is increased because of the electric layer. Since the coastal waters are enriched in organic matter effluents and chemical process liquids, the natural surface film forms a complex molecular structure. A particular role is played by organic matter of surface-active properties.

Surface entropy decreases with an increase in surface adsorption of the amphiphiles (Yamabe et al., 2000). In other words, the surface adsorption from the bulk solution brings about larger negative entropy change.  $S_s$  values were higher for all the studied samples that suggested the negative adsorption effect as a characteristic phenomenon for electrolytes applicable to only pure surface adsorption mechanism (Adamson and Gast, 1997).

However, for the natural sea surface films consisting of polymer-like structures, the thermodynamic and kinetic processes are more complex (Gelbart et al., 1994). Higher values of  $S_s$  pointed to the less-organized molecular interfacial structure in reference to the seawater data. Application of 2D polymer film scaling theory to natural sea surface films allowed expressing the structural complexity of the interfacial region with the scaling parameter  $\gamma$  (Pogorzelski, 1996). It was

**Table 1** Surface tension, surface entropy, surface enthalpy, and surface specific heat, for Baltic Sea water samples.

No.	Site (date)	$\gamma_{AW}$ [ $\text{mN m}^{-1}$ ]	$S_s$ [ $\text{mN m}^{-1} \text{K}^{-1}$ ]	$TS_s$ [ $\text{mN m}^{-1}$ ]	$H_s$ [ $\text{mN m}^{-1}$ ]	$C_s$ [ $\text{mN m}^{-1} \text{K}^{-1}$ ]	$T$ [K]
1	Gdynia-boulevard 17 April 2013	75.9 (0.1)	0.146 (0.008)	41.24 (2.35)	117.14 (5.85)	−0.0080	280.6 (0.1)
2	Gdynia-Orłowo 17 April 2013	76.5 (0.1)	0.149 (0.004)	41.94 (1.39)	118.44 (5.92)	−0.0025	280.6 (0.1)
3	Sopot 17 April 2013	76.7 (0.1)	0.203 (0.007)	57.13 (2.15)	133.8 (6.69)	−0.0044	280.6 (0.1)
4	Jelitkowo 17 April 2013	77.0 (0.1)	0.179 (0.004)	50.43 (1.29)	127.43 (6.37)	−0.0141	280.6 (0.1)
5	Brzeźno 17 April 2013	77.4 (0.1)	0.199 (0.007)	55.85 (2.12)	133.25 (6.66)	−0.0153	280.6 (0.1)
6	Pure water (distilled)	74.59	0.157	44.06	118.65	−0.0175	280.66 <sup>a</sup>
7	Seawater of 6 PSU salinity	74.69	0.144	40.42	115.11	−0.0163	280.66

Standard deviation given in brackets.

<sup>a</sup> The long-term average sea surface temperature in the Baltic Sea.

derived from the Langmuir trough surface pressure–area studies according to the relation  $E_{isoth} = \gamma\pi$ . An increase in  $\gamma$  from  $<3.5$  through  $\sim 8$  to over 10 indicating “good”,  $\theta$ , and “poor” solvent behavior, respectively of the interfacial system, is correlated with the structure transition in the multi-component film beginning from a homogeneous mixed (of lowest organization state) monolayer, through a heterogeneous film with SAS substances segregated into patches or domains to at least a vertically layered structure with the most insoluble components residing on top of the microlayer. The scaling exponent  $\gamma$  is a complex function of environmental factors affecting film structure (SAS concentration, pH, ionic strength and composition of the subphase, temperature, locations of sampling site and film collection procedure). Values of  $\gamma$  measured at the studied locations were Gdynia (8.1), Gdynia-Orłowo (7.3), Sopot (3.7), Jelitkowo (6.2) and Brzeźno (4.2).

At the same place (Jelitkowo),  $\gamma$  varied from 3.7 to 7.9 in the summer time (May–September) to 10–12.6 in the winter months (January, February, November, December), reflecting the film structure evolution from the less to more organized state. It can be noted that higher  $S_s$  were correlated to lower  $\gamma$  registered in the studied stations (see Table 1). The entropic term  $TS_s$  contributions to the surface enthalpy  $H_s$  were varied from 0.35 to 0.42 and were higher if referred to the seawater reference (= 0.34) reflecting the presence of the adsorbed species. Surface specific heat  $C_s$  of the studied samples was ranging from  $-0.004$  to  $-0.015$   $\text{mN m}^{-1} \text{K}^{-1}$  and was much lower than the reference value  $-0.016$   $\text{mN m}^{-1} \text{K}^{-1}$  suggesting the less sensitivity of the natural interfacial seawater system to temperature variations.

Seasonal changes of the surface thermodynamics parameters followed at the particular station, i.e. Gdynia-Orłowo in the period 30 November 2012 to 29 November 2013, are summarized in Table 2.

The presented parameters varied widely:  $\gamma_{AW}$  from 69.9 to 76.5  $\text{mN m}^{-1}$ ;  $S_s = 0.130$ – $0.685$   $\text{mN m}^{-1} \text{K}^{-1}$ ;  $H_s = 111.07$ – $264.01$   $\text{mN m}^{-1}$ . This is an example of a particular coastal area with freshwater influence (Kacza River) and municipal effluents which can screen the effect of natural waters enrichment by seasonal biological activity matter. Usually

observed lower  $\gamma_{AW}$ ,  $\gamma$  and higher  $S_s$ ,  $E_{isoth}$  noticed in the summer time as a general trend along the coastal areas of the Baltic Sea was not evidenced here (Pogorzelski and Kogut, 2003). Seasonal variability of  $\gamma$  and  $S_s$  for Baltic Sea water samples is shown in Fig. 5a and b, respectively registered at the selected sites. The smallest surface tension deviations from the reference value =  $74.69$   $\text{mN m}^{-1}$  were observed at the period of limited primary production in winter season months (November to February). In the summer time both the human activity and marine organisms surface active compounds adsorb at the air/water interface. The effect is less pronounced in the locations distant from industrial objects (Gdynia-boulevard, Sopot).  $S_s$  being a first derivative of  $\gamma$  against  $T$  is a very sensitive quantity of the water season kind. A slight deviation from the reference was noticed from November 2012 to April 2012, further from May 2012 to October 2013,  $S_s$  differed by a factor of 5.8–7.6 exhibited a drastic structural re-arrangement at the interface again less pronounced at Gdynia-boulevard and sampling stations where lowest SAS concentrations were evidenced in previous studies (Pogorzelski et al., 2006).

The establishment of the thermodynamic equilibrium in the film is not trivial. The effect depends on the dimensionless parameter Deborah number. The interfacial system appears to be at the quasi-equilibrium thermodynamic state if  $De$  number is less than unity. In order to evaluate the film formation rate of the equilibrium state, the adsorptive properties of film-forming by surface active substances have to be considered.

In the surface microlayer of natural waters, a great diversity of SAS organic substances has been observed. Besides proteins and glycerides, characterized by small surface activity, there are also very active esters, fatty acids, and alcohols (Jarvis et al., 1967). The latter stands for main components of the surface layer as a result of competitive adsorption (Garrett, 1967). They consist of molecules having between 11 and 22 carbon atoms in a hydrocarbon chain. The elasticity modulus of condensed monolayers of this type may reach a value of  $200$   $\text{mN m}^{-1}$  ( $\text{C}_{20}\text{H}_{41}\text{OH}$  – see Joly, 1972). The surface adsorption parameters characterizing several selected organic surface-active substances occurring on

**Table 2** Seasonal variability of the surface thermodynamics parameters of Baltic Sea water samples collected at Gdynia-Orłowo from 30 November 2012 to 29 November 2013 corrected to the reference temperature.

No.	Date	$\gamma_{AW}$ [ $\text{mN m}^{-1}$ ]	$S_s$ [ $\text{mN m}^{-1} \text{K}^{-1}$ ]	$TS_s$ [ $\text{mN m}^{-1}$ ]	$H_s$ [ $\text{mN m}^{-1}$ ]
1	30 November 2012	72.6 (0.1)	0.260 (0.010)	72.95 (2.81)	145.55 (7.26)
2	28 December 2012	73.5 (0.1)	0.191 (0.004)	53.59 (1.12)	127.09 (6.35)
3	31 January 2013	75.1 (0.1)	0.184 (0.005)	51.63 (1.40)	126.73 (6.33)
4	23 February 2013	75.3 (0.1)	0.167 (0.003)	46.86 (0.84)	122.16 (6.11)
5	27 March 2013	74.6 (0.1)	0.130 (0.020)	36.47 (5.61)	111.07 (5.55)
6	17 April 2013	76.5 (0.1)	0.149 (0.004)	41.81 (1.12)	118.31 (5.92)
7	28 May 2013	74.7 (0.1)	0.245 (0.010)	68.74 (2.81)	143.44 (7.17)
8	29 June 2013	74.7 (0.1)	0.221 (0.006)	62.01 (1.68)	136.71 (6.83)
9	13 July 2013	72.0 (0.1)	0.579 (0.011)	162.46 (3.09)	234.46 (11.72)
10	10 August 2013	71.8 (0.1)	0.685 (0.029)	192.21 (8.13)	264.01 (13.20)
11	22 September 2013	71.3 (0.1)	0.531 (0.014)	148.99 (3.92)	220.29 (11.01)
12	27 October 2013	69.9 (0.1)	0.744 (0.055)	208.76 (15.43)	278.66 (13.93)
13	29 November 2013	75.2 (0.1)	0.145 (0.007)	40.69 (1.96)	115.88 (5.79)

Standard deviation given in brackets.

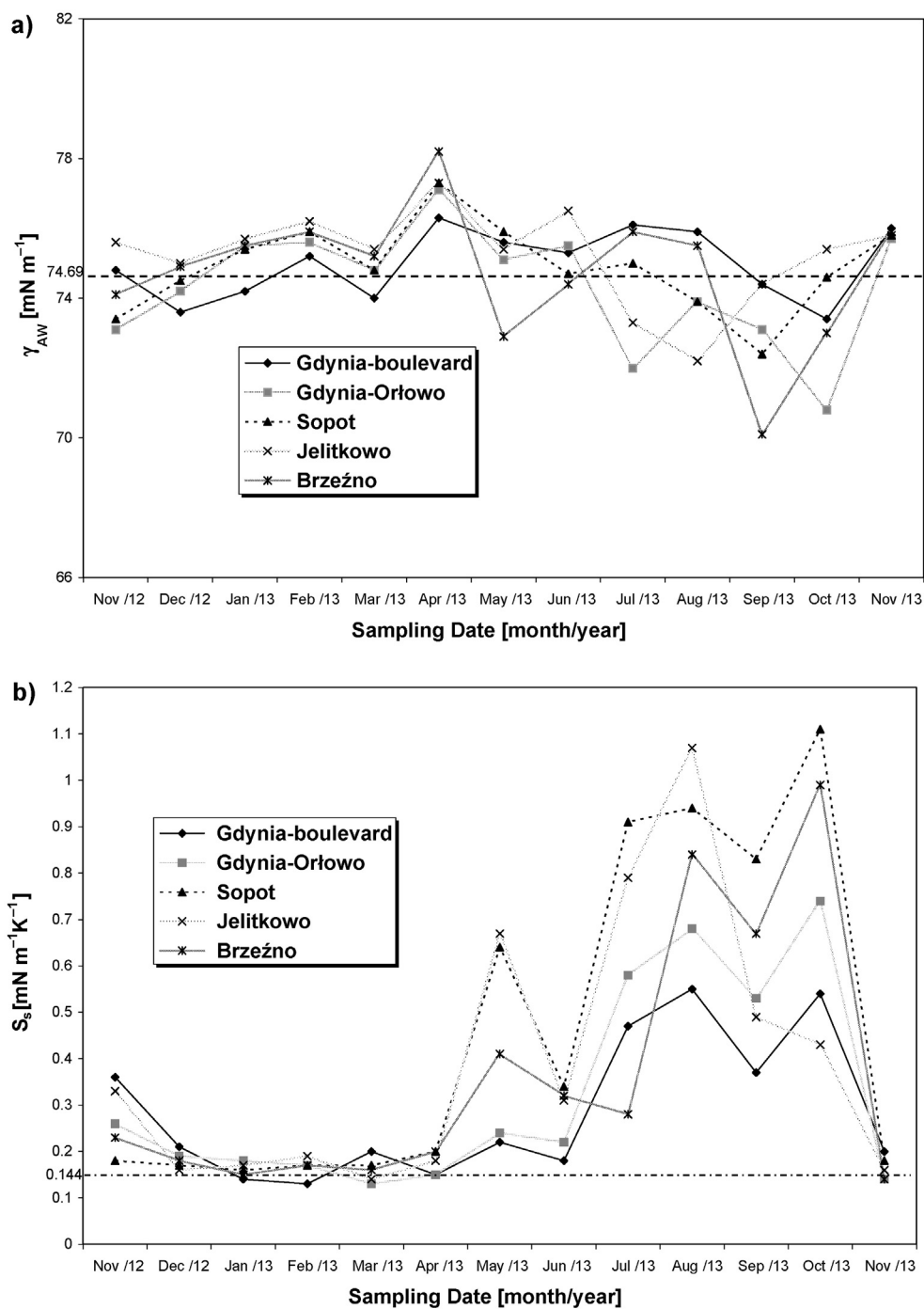


**Figure 5** Seasonal variability of surface tension (a) and surface entropy (b), for Baltic Sea water samples collected at the selected locations sampled in the period from November 2012 to November 2013. Horizontal lines correspond to the reference values.

**Table 3** Surface adsorption parameters of SAS composing the sea surface films.

Substance	$a$ [kmol m <sup>-3</sup> ]	$\Gamma_{\infty}$ [kmol m <sup>-2</sup> ]	$D$ [m <sup>2</sup> s <sup>-1</sup> ]	$t_r$ [s]
C <sub>7</sub> H <sub>15</sub> COOH	$1.2 \times 10^{-3}$	$2 \times 10^{-9}$	$1.1 \times 10^{-10}$	0.00049
C <sub>12</sub> H <sub>25</sub> SO <sub>4</sub> Na	$4.4 \times 10^{-4}$	$5.7 \times 10^{-9}$	$7.3 \times 10^{-10}$	0.00284
C <sub>10</sub> H <sub>21</sub> OH	$1.4 \times 10^{-3}$	$6.1 \times 10^{-9}$	$3.7 \times 10^{-10}$	10.3375
C <sub>12</sub> H <sub>25</sub> OH	$4.3 \times 10^{-6}$	$7 \times 10^{-9}$	$6 \times 10^{-10}$	54.5291
C <sub>11</sub> H <sub>23</sub> COOH	$1.4 \times 10^{-6}$	$6 \times 10^{-9}$	$7.4 \times 10^{-10}$	306.4293



the surface of natural waters, together with the characteristic relaxation times (derived from Eq. (9)) are collected in Table 3, for the state of saturated adsorption monolayer ( $c = 2a$ ). In the case of readily soluble substances ( $a = 10^{-3} - 10^{-4} \text{ kmol m}^{-3}$ ), diffusion is a very fast process with  $t_r$  of the order of 0.49–2.84 ms. Substances having the activity coefficient  $a = 10^{-6} \text{ kmol m}^{-3}$  and lower form effectively insoluble monolayers within the time window range of the order of several seconds to minutes demonstrating  $t_r$  ranging from 10 to 306 s.

The foreseen effect of interfacial film time formation on the sea surface thermodynamic parameters was confirmed experimentally by using a gas-bubble tensiometer with the adjustable bubble surface formation age  $t_b$ . Surface tension and  $S_s$  were equal to  $75.1 \text{ mN m}^{-1}$  and  $0.189 \text{ mN m}^{-1} \text{ K}^{-1}$  for the time  $t_b = 28 \text{ ms}$  whereas  $74.7 \text{ mN m}^{-1}$  and  $0.214 \text{ mN m}^{-1} \text{ K}^{-1}$  for  $t_b = 275 \text{ ms}$  on Baltic Sea sample measured in situ at Orłowo on 28 May 2013. The following trend of changes:  $\gamma \downarrow$  and  $S_s \uparrow$  with an increase of  $t_b$  was found for all the studied samples.

Under high sea states intensive water mixing takes place where subsurface water phase of different SAS content accounts in the surface film formation. That was simulated by surface tension measurements of seawater probes taken from different depths.

Surface tension of seawater as a function of time registered from the moment of creation of air/water interface, for water phases collected with a microlayer sampler and in bottles from subsurface water from depths 0.5, 1.0 and 1.5 m, is shown in Fig. 6. Measurements were performed on water samples collected at Jelitkowo on 12 May 2013 under calm sea conditions ( $V_{10} < 2 \text{ m s}^{-1}$ ).

The lowest value of  $\gamma$  was observed for the at-surface microlayer case ( $h = 0$ ) in comparison to the reference value for pure (surfactant-free) water  $\gamma = 74.8 \text{ mN m}^{-1}$  at the sample temperature  $T = 6.0^\circ\text{C}$  as a result of SAS adsorption.

The corresponding film pressure attained  $\pi = 8.3 \text{ mN m}^{-1}$ , i.e. the equilibrium value after  $t = 65 \text{ min}$ . During this period  $\gamma$  evolved from  $65.5$  to  $66.5 \text{ mN m}^{-1}$ . The subsurface water under stable hydrodynamic conditions (no water mixing) contained lower concentrations of surface-active components that is expressed by higher values of  $\gamma$  taken for samples collected from deeper layers:  $\gamma = 69.1 \text{ mN m}^{-1}$  ( $h = 0.5 \text{ m}$ );  $\gamma = 74.1 \text{ mN m}^{-1}$  ( $h = 1.0 \text{ m}$ ), and  $\gamma = 74.4 \text{ mN m}^{-1}$  ( $h = 1.5 \text{ m}$ ). The subsurface water samples were capable of forming films with low  $\pi$  varying from  $5.7$  ( $h = 0.5 \text{ m}$ ) to  $0.4$  ( $h = 1.5 \text{ m}$ ). The surface-active components appeared to be slightly soluble compounds at low concentrations, for which the diffusion process required several minutes (or even hours) to attain the constant  $\gamma$  value. It can be noted that  $\gamma$ - $t$  dependence did not demonstrate a horizontal part corresponding to the saturation value, for the deep-water samples ( $h = 1.0 - 1.5 \text{ m}$ ). Surfactants are concentrated at the air-sea interface by numerous physical processes including diffusion, turbulent mixing, bubble and particle transport, and convergent circulations driven by wind, tidal forces, and internal waves. Natural sea surface films most resemble layers composed of proteins, polysaccharides, humic-type materials and waxes (Van Vleet and Williams, 1983). The presence of relatively small amounts of certain lipids (free fatty acids, free fatty alcohols or triglycerides) in films composed primarily of proteins or carbohydrates can strongly affect the resultant film pressure of multicomponent film. The elastic behavior of sea surface films is not only controlled by diffusion and compounds concentrations, but also by pronounced conformational changes (Gelbart et al., 1994). Consequently, losses of film material could have occurred via desorption, micelle formation, or collapse to a multilayered solid phase. Conformation mechanisms could include more efficient packing due to nonpolar interactions, coiling of biopolymer chains, and looping of polymer segments into bulk solution. The

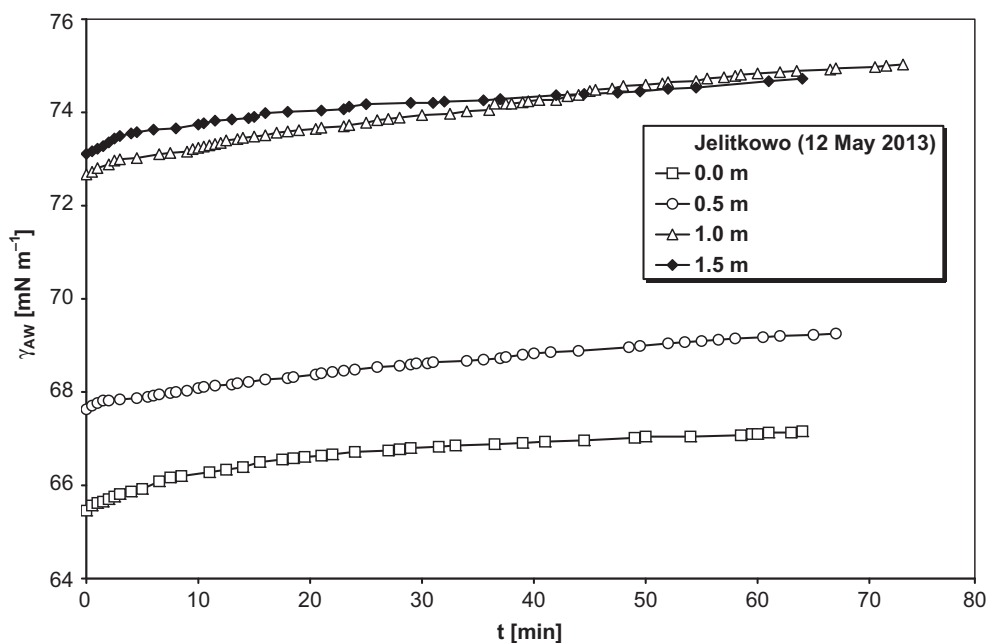


**Figure 6** Dynamic surface tension  $\gamma(t)$ , for seawater samples collected with a surface film sampler and in bottles from different depths 0.5, 1.0 and 1 m (at Jelitkowo on 12 May 2013).

**Table 4** Physicochemical properties of crude oils used in the experiments at 25°C.

No.	Crude oil	Petrobaltic	Flotta	Romashkino
1	Density [kg m <sup>-3</sup> ]	806.88	874.83	848.01
2	Viscosity [mPa s]	5.17	6.57	4.71
3	Surface tension [mN m <sup>-1</sup> ]	25.74	28.04	25.76
4	O/W Interfacial tension <sup>a</sup> [mN m <sup>-1</sup> ]	20.52	21.64	22.54
5	API	43.48	29.88	34.99
6	Pour point	-5	-2	-3
7	Asphaltenes [%w/w]	1.4	0.7	0.4
8	Resins [%w/w]	6.3	5.1	4.2
9	Classification	Light	Medium	Light
10	Origin	Baltic Sea	North Sea (UK)	Russia

<sup>a</sup> Crude oil in contact with Baltic Sea water sample (collected at Orłowo on 25 May 2013).

glycopeptides-lipid-oligosaccharide complex, such as that described by D'Arrigo (1984), appears to be more consistent with the observations of surface characteristics of marine films found in the Baltic Sea (Pogorzelski et al., 2006).

#### 4.2. Interfacial thermodynamics of A/O and O/W crude oil-seawater systems

Physicochemical properties of crude oils used in the experiments (at 25°C), are collected in Table 4, and were characteristic of light to medium oils.

Interfacial thermodynamic functions for A/O and O/W systems are shown in Table 5. Surface tension of the studied crude oils and interfacial SW/oil tensions were comparable to the values reported by others (Mohammed et al., 1993; Nour et al., 2008; Yarranton et al., 2000).  $S_s$  of A/O interfaces was close to the values of long-chain paraffin oils (Birdi, 1997a, 1997b), and were higher by a factor 2.1–3.9 in reference to O/W interfaces, for the corresponding crude oil. It demonstrated that the interfacial molecular structure, for O/W systems, was more structurally ordered (of lower degrees of freedom) than exhibited by A/O interfaces for the same crude oil. It remains to better understand the surface activity of asphaltenes and resins – the main surface-active components of crude oil affecting  $\gamma_{AW}$  and  $\gamma_{OW}$  interfacial tensions (Bauget et al., 2001). Resin and asphaltene contents of the studied crude oils are of the order of 4.2–6.3 and 0.4–1.4 [wt%], respectively similarly as reported in Freer et al. (2003). The effect of concentrations of asphaltenes and resins on static and dynamic

properties of air/oil and water/oil interfaces was already experimentally studied (Ese et al., 1999). The experimental data indicate that, at low concentrations, asphaltenes adsorb on the water-in-hydrocarbon interface as surfactants (Yarranton et al., 2000). Sandwich structures at oil-water interface are observed (Horvath-Szabo et al., 2002). Recent molecular dynamics simulation of the oil-water interface reveals a preferential accumulation of aromatics at the interface due to weak hydrogen bonding between hydrogen atoms of water and  $\pi$ -electrons of aromatics (Kunieda et al., 2010). Detailed discussion on the correlation between the chemical composition of the crude oil and interfacial tension can be found in Buckley and Fan (2007). Aromatics that are preferentially accumulated at the crude oil/water interface will promote migration of asphaltenes and polar components in the crude oil toward the interface, resulting in further reduction in the interfacial tension between crude oil and seawater to below 30 mN m<sup>-1</sup> (Takamura et al., 2012). The generalized model that relates interfacial tension of crude oil/brine systems with temperature, salinity and oil viscosity is given by the equation (Isehunwa and Olanisebe, 2012):  $\gamma_{OW} = A + BX_1 + CX_2 + DX_3$  where  $X_1$  is the temperature [°C],  $X_2$  the salinity [ppm],  $X_3$  the oil viscosity [cP] with the empirical constants A–D collected in Table 2 of Isehunwa and Olanisebe (2012) designed for the particular crude oil system. Other important factors like pH are also considered (Olanisebe and Isehunwa, 2013).

The adsorption process at the air/oil interface is not diffusion controlled but rather involves a reorganization of asphaltene molecules in a network structure. The role of

**Table 5** Surface thermodynamic parameters of A/O and O/W interfacial system crude oil–seawater at 25°C.

No.	Oil phase	$\gamma_{AO}$ [mN m <sup>-1</sup> ] at $T = 295$ K	$S_s$ [mN m <sup>-1</sup> K <sup>-1</sup> ]	$TS_s$ [mN m <sup>-1</sup> ]	$H_s$ [mN m <sup>-1</sup> ]	$C_s$ [mN m <sup>-1</sup> K <sup>-1</sup> ]	$T$ [K]
<b>A/O interface</b>							
1	Crude oil (Petrobaltic)	25.74 (0.28)	0.188 (0.006)	53.33 (1.88)	104.43 (5.22)	-0.137 (0.006)	283 (0.1)
2	Crude oil (Flotta)	28.04 (0.40)	0.141 (0.009)	41.34 (2.62)	90.24 (4.51)	-0.157 (0.007)	292 (0.1)
3	Crude oil (Romashkino)	25.76 (0.29)	0.159 (0.010)	47.53 (2.99)	76.93 (3.84)	-0.108 (0.005)	298 (0.1)
<b>O/W interface</b>							
4	SW/Petrobaltic	20.52 (0.18)	0.048 (0.010)	13.58 (1.32)	34.10 (0.23)	-0.241 (0.012)	283 (0.1)
5	SW/Flotta	21.64 (0.21)	0.065 (0.014)	18.98 (1.96)	40.62 (0.35)	-0.617 (0.027)	292 (0.1)
6	SW/Romashkino	22.54 (0.11)	0.057 (0.012)	16.99 (1.87)	39.53 (0.33)	-0.715 (0.032)	298 (0.1)

SW, Baltic Sea water sample (collected at Orłowo on 25 May 2013). Standard deviation given in brackets.

**Table 6** Rheokinetic surface parameters derived from stress-relaxation experiments at 25°C for A/W, A/O and O/W interfaces.

No.	Sample date	$\Delta A/A_0$	$\Delta t$ [s]	$\tau_1$ [s]	$\tau_2$ [s]	$E_{isoth}$ [mN m <sup>-1</sup> ]	$E_d$ [mN m <sup>-1</sup> ]	$E_i$ [mN m <sup>-1</sup> ]	$ E $ [mN m <sup>-1</sup> ]	$\varphi$ [°]
1	Brzeźno 12 July 2013	0.13 (0.01)	0.4	2.0 (0.2)	21.9 (2.6)	29.12 (3.49)	12.03 (1.44)	3.72 (0.44)	12.59 (1.51)	17.1 (2.1)
2	Jelitkowo 29 June 2013	0.12 (0.01)	0.7	2.4 (0.3)	12.2 (1.5)	25.81 (3.09)	16.98 (0.83)	4.45 (0.29)	17.55 (0.88)	14.6 (2.3)
3	Orłowo 15 July 2013	0.08 (0.01)	0.3	1.6 (0.2)	10.1 (1.2)	24.48 (2.93)	17.58 (2.11)	5.31 (0.63)	18.37 (2.20)	16.8 (2.0)
4	Sopot 23 August 2013	0.08 (0.01)	0.4	2.0 (0.2)	10.2 (1.2)	23.12 (2.77)	18.55 (1.62)	4.18 (0.50)	19.01 (1.70)	12.6 (2.1)
5	Gdynia 18 June 2013	0.11 (0.01)	0.6	2.8 (0.2)	12.3 (1.1)	22.94 (1.89)	16.89 (1.22)	4.36 (0.9)	17.44 (1.41)	14.3 (1.8)
6	Petrobaltic A/O	0.12 (0.02)	0.7	1.9 (0.1)	23.2 (4.5)	3.42 (0.45)	1.06 (0.12)	0.42 (0.32)	1.55 (0.34)	21.6 (1.9)
7	Flotta A/O	0.12 (0.02)	0.7	2.0 (0.1)	27.7 (2.3)	2.78 (0.67)	0.81 (0.11)	0.34 (0.32)	0.88 (0.21)	22.7 (1.7)
8	Romashkino A/O	0.13 (0.02)	0.6	2.7 (0.1)	31.1 (2.4)	3.2 (0.82)	1.96 (0.12)	0.85 (0.37)	2.13 (0.26)	23.4 (1.7)
9	Petrobaltic SW/O	0.19 (0.02)	0.5	3.6 (0.2)	28.2 (3.4)	13.62 (2.71)	8.81 (1.62)	4.10 (0.21)	9.71 (0.13)	24.9 (2.3)
10	Flotta SW/O	0.23 (0.02)	0.4	5.2 (0.3)	35.7 (4.03)	10.24 (3.23)	7.93 (1.40)	3.87 (0.56)	8.82 (0.11)	26.1 (2.8)
11	Romashkino SW/O	0.23 (0.02)	0.6	7.3 (0.3)	42.7 (4.06)	15.43 (4.77)	10.12 (2.45)	5.32 (0.42)	11.43 (0.23)	27.7 (3.6)

resins, another crude oil surface-active component is also important: resins are through to pack around asphaltene aggregates making them more soluble in the oil and therefore less surface active. Surface tension of alkanes is a result of London dispersion interactions, which are directly proportional to density. When the surface tensions of a series of the crude oils is plotted versus their densities, they follow a close-to-linear relationship but the values fall significantly below those for alkanes of the same density due to preferential accumulation of light end alkanes at the crude oil surface. The formation of a solid skin at air/oil interfaces is well identified by an increase of the elastic modulus, as will be argued in the next section.

The entropy contribution term related to the interface creation represented 51–62% of  $H_s$ , for A/O interfaces, and less 39–46, for O/W interfaces comparable to the one noticed for A/W interfaces (see Table 5). The molecular structure of SAS at the interface between two immiscible phases depends on the phase dielectric constants. The ratio of these constants are equal to 1/80 (A/W), 4/80 (O/W) and only 1/4 (A/O). More condensed surfactant 2D monolayer phases (of lower structural entropy) are formed at A/W interfaces in reference to the O/W interface where more expanded and less structured films are obtained, for the particular SA component (Adamson and Gast, 1997).  $|C_s|$  values for O/W interfaces were higher by a factor 2–7 in reference to the A/O interface that exhibited their lower heat capacity.

### 4.3. Interfacial viscoelasticity

Force-area isotherm and stress-relaxation studies performed on Baltic Sea water samples in contact with crude oils allowed the surface viscoelastic A/O and SW/O interfacial parameters to be determined, as collected in Table 6.

Natural seawater film studies revealed, in stress-surface pressure relaxation measurements, a two-step relaxation process with characteristic times  $\tau_1$  (1.6–2.8 s) and  $\tau_2$  (10.1–21.9 s) being in agreement with the previous data obtained in the same coastal areas (Table 2 of Pogorzelski and Kogut (2003)). They also demonstrated that we were concerned with not purely elastic films ( $E_d > E_i$ ) with the loss angles ranging from 12.6 to 17.1°. At the applied film area compression velocities, as adopted in these stress-interface studies,  $De$  parameter was not lower than unity, even if the shorter  $\tau_1$  was taken. The interfacial system was not in its quasi-equilibrium thermodynamic state. As a result, the absolute value of the complex modulus  $E$  (i.e.  $|E| = (E_d^2 + E_i^2)^{1/2}$ ) could not be approximated by the static elasticity  $E_{isoth}$ . For all the studied surfaces  $E_{isoth} > |E|$ , that exhibited the need for a proper selection of  $E$  values in any simulations of dynamical processes at interfaces (wind waves damping and generation, crude oil spreading, etc.).  $E_{isoth}$  values derived from the force-area isotherm studies turned out to be overestimated. The viscoelasticity of the remaining surfaces both A/O and O/W pointed to the viscoelastic behavior where  $E_i$  differed from  $E_d$  by a factor 2.3–2.5, for A/O and by 1.9–2.14, for O/W interfaces with higher  $\varphi = 21.6$ –27.7° in reference to A/W surfaces (=12.6–17.1°).  $|E|$  values were much lower for O/W (9.71–11.43) and A/O (0.88–2.13) than measured for Baltic Sea water (12.59–19.01 mN m<sup>-1</sup>).

Resin and asphaltene contents of original crude oils are of the order of 24–26 and 2.6–3.9 [wt%], respectively (Freer et al., 2003). The effect of concentrations of asphaltenes of resins on static and dynamic properties of air/oil and water/oil interfaces was already experimentally studied (Ese et al., 1999). The formation of a solid skin at air/oil interfaces is well identified by an increase of the elastic modulus. After a sufficiently long time (less than 1 week) the elasticity modulus  $E_{AO}$  can grow from its initial value ( $= 0.5 \text{ mN m}^{-1}$  shortly after the air/oil interface formation) to 10–20  $\text{mN m}^{-1}$  (Bauget et al., 2001).

The overall relaxation kinetics of a compressed air–oil interface and the resulting dynamic elasticity  $E$  was studied for two crude oil derivatives (Loglio et al., 1984). The stress-relaxation method, at the applied area strain rate,  $(\Delta A/A)/\Delta t = 0.183 \text{ s}^{-1}$  in a Langmuir trough, revealed a single relaxation process with long relaxation times  $\tau_R = 623 \text{ s}$  and  $1,248 \text{ s}$ , with low values of viscoelasticity modulus  $|E|$  equal to  $2.8 \text{ mN m}^{-1}$  and  $3.3 \text{ mN m}^{-1}$ , for diesel and boiler oil, respectively. It was found for two crude oils immersed in synthetic sea water, the O/W interface behaves primarily elastically (the interfacial loss modulus  $E_i < 4 \text{ mN m}^{-1}$  is smaller than the interfacial storage modulus  $E_d < 10 \text{ mN m}^{-1}$ ) and that more asphaltenic the oil the stronger is the interfacial elas-

ticity (Freer et al., 2003). Moreover, interfacial O/W elasticity grows slowly in time over days and is clearly manifest even when “rigid skins” are not visible to the eye. Formation of such “skins” at the oil/water interface with significant mechanical strength demands interconnection of a growth into large-scale network structures. These structures are expected to evolve slowly that could lead to another oil spreading rate-limiting mechanism, for instance (Boniewicz-Szmyt and Pogorzelski, 2008).

#### 4.4. Elasticity of composite seawater–oil interface

The apparent modulus  $E_{com}$  of the composite surface consisting of different homogeneous parts (i.e. oil-covered and oil-free water surfaces) can be derived from the relation (Ravera et al., 2005):

$$\frac{1}{E_{com}} = \frac{F_1}{E_1} + \frac{F_2}{E_2} + \dots + \frac{F_n}{E_n} = \sum_{i=1}^n \frac{F_i}{E_i}. \quad (16)$$

Here  $F_i = A_i/A_{tot}$  and  $E_i$  represent the area fraction of the total surface  $A_{tot}$  ( $\sum F_i = 1$ ), and dilational elasticity modulus of  $i$ th component occupying  $A_i$  area, respectively.

For our case considered here, crude oil lenses covering a certain area of seawater as shown in Fig. 7, we need to know the fraction of the total area occupied by oil ( $F_0$ ) and dilational modulus  $E_{O/W}$  attributed to such a part, in general  $E_O = E_{O/W} + E_{AO}$  (modulus  $E_{AO}$ , for the air/oil interface is rather small (see Table 6) and often assumed as 0). The remaining oil-free surface has the modulus  $E_{AW}$  with the area fraction  $F_{AW} = 1 - F_0$ . As a result, we have:

$$\frac{1}{E_{com}} = \frac{F_0}{E_{OW}} + \frac{(1 - F_0)}{E_{AW}}. \quad (17)$$

The theoretical  $E_{com}$  value was calculated from Eq. (17) with the following input values:  $E_{AW} = 28.8 \text{ mN m}^{-1}$ ,  $E_{OW} = 13.6 \text{ mN m}^{-1}$ ,  $E_{AO} = 3.4 \text{ mN m}^{-1}$  ( $E_O = 17.0 \text{ mN m}^{-1}$ ) and  $F_0 = 0.33$  was equal to  $23.4 \text{ mN m}^{-1}$ . The experiment demonstrated similar  $E_{com} = 26.6 \text{ mN m}^{-1}$  being in agreement within 12%. The presence of an oil lens at natural surfactant-covered sea surface leads to a significant drop of  $E$  (from  $E_{AW}$  to  $E_{com}$ ) even for low oil coverage ( $F_0 < 0.1$ ).

## 5. Conclusions

Thermodynamic properties of seawater studied in Baltic Sea coastal waters differ significantly from the reference literature data and exhibited location-specific, seasonal and temporal variability likely related to the surface-active organic matter fraction of natural and man-made origin.

The measured surface tension and interfacial tension temperature dependences allowed correcting surface thermodynamic data to the desired temperature range.

For the first time temperature dependences of AO and OW interfaces for seawater in contact with model crude oils were measured as well as the elasticity modules. All the studied interfaces turned out to be viscoelastic with the characteristic relaxation times of the order of several seconds, and the absolute modules were found to follow the order:  $E_{AW} > E_{OW} \gg E_{AO}$ .

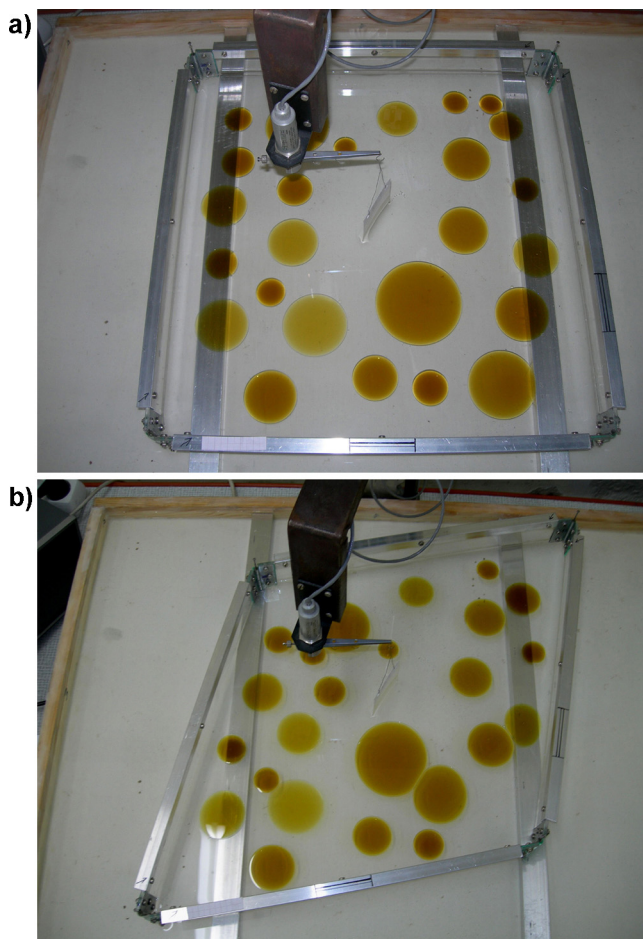


**Figure 7** Composite crude oil (Petrobaltic) lenses-seawater (Baltic Sea water from Orłowo station) surface studied in a frame-type Langmuir trough (a) before and (b) after short pulse ( $\Delta t = 0.5 \text{ s}$ ); area compression  $\Delta A/A_0 = 0.08$  and  $F_0 = 0.33$ .



For the composite crude oil/seawater contaminated surface, the elasticity modulus was significantly lowered even for a low covering fraction  $F_0$  of lens-shaped areas.

The obtained data are essential to test the corrected model of crude oil kinetics spreading at sea proposed by the authors where the dynamic spreading coefficient instead of the static one was postulated (Boniewicz-Szmyt and Pogorzelski, 2008).

## References

- Adamson, A.W., Gast, A.P., 1997. *Physical Chemistry of Surfaces*, 6th ed. Wiley and Sons, NY.
- Aksenenko, E.V., Kovalchuk, V.I., Fainerman, V.B., Miller, R., 2006. Surface dilational rheology of mixed adsorption layers at liquid interfaces. *Adv. Colloid Interface Sci.* 122, 57–66.
- Bauget, F., Langevin, D., Lenormand, R., 2001. Dynamic surface properties of asphaltenes and resins at the oil–water interface. *J. Colloid Interface Sci.* 239, 501–508.
- Birdi, K.S., 1997a. Surface crystallization of hexadecane at hexadecane/air and hexadecane/water interfaces and effect of proteins. *Colloids Surf. Physicochem. Eng. Aspects* 123–124, 543–548.
- Birdi, K.S., 1997b. Prediction of critical temperature of n-alkanes and n-alkenes from surface tension vs. temperature data. *Colloid Polym. Sci.* 275, 561–566.
- Boniewicz-Szmyt, K., Pogorzelski, S.J., 2008. Crude oil derivatives on sea water: signatures of spreading dynamics. *J. Mar. Syst.* 74, 541–551.
- Boniewicz-Szmyt, K., Pogorzelski, S.J., 2015. Mineral dust particles effect on viscoelasticity of seawater: Baltic Sea case studies. *Mar. Environ. Res.* (submitted).
- Buckley, J.S., Fan, T., 2007. Crude oil/brine interfacial tensions. *Petrophysics* 48, 175–185.
- Butt, H.-J., Graf, K., Kappl, M., 2003. *Physics and Chemistry of Interfaces*. Wiley-VCH Verlag & Co., New York.
- Cini, R., Loglio, G., Ficalbi, A., 1972. Temperature dependence of the surface tension of water by the equilibrium ring method. *J. Colloid Interface Sci.* 41, 287–297.
- D'Arrigo, J.S., 1984. Surface properties of microbubble-surfactant monolayers at the air/water interface. *J. Colloid Interface Sci.* 100, 106–111.
- Druffel, E.R.M., Bauer, J.E., 2000. Radiocarbon distributions in Southern Ocean dissolved and particulate organic matter. *Geophys. Res. Lett.* 27, 1495–1498.
- Ese, M.-H., Galet, L., Clause, D., Sjoblom, J., 1999. Properties of Langmuir surface and interfacial films built up by asphaltenes and resins: influence of chemical demulsifiers. *J. Colloid Interface Sci.* 220, 293–301.
- Freer, E.M., Svitova, T., Radke, C.J., 2003. The role of interfacial rheology in reservoir mixed wettability. *J. Petrol. Sci. Eng.* 39, 137–158.
- Garrett, W.D., 1967. The organic chemical composition of the ocean surface. *Deep Sea Res. Oceanogr. Abstr.* 14, 221–227.
- Gelbart, W.M., Ben-Shaul, A., Roux, D. (Eds.), 1994. *Micelles, Membranes, Microemulsions and Monolayers*. Springer-Verlag, New York, p. 608.
- Harkins, W.D., 1952. *The Physical Chemistry of Surface Films*. Reinhold, New York.
- Horvath-Szabo, G., Czarnecki, J., Masliyah, J.H., 2002. Sandwich structures at oil–water interfaces under alkaline conditions. *J. Colloid Interface Sci.* 253, 427–434.
- Hunter, K.A., Liss, P.S., 1981. Organic sea surface films. In: Duursma, E.K., Dawson, R. (Eds.), *Marine Organic Chemistry*. Elsevier Oceanography Series 31, New York, 259–298.
- Isehunwa, S.O., Olanisebe, E.B., 2012. Interfacial tension of crude oil-brine systems in the Niger delta. *Int. J. Recent Res. Aspects* 10, 460–465.
- Jarvis, N.L., Garrett, W.D., Scheiman, M.A., 1967. Surface chemical characterization of surface active material in sea surface. *Limnol. Oceanogr.* 12, 88–96.
- Jayalakshmi, Y., Ozanne, L., Langevin, D., 1995. Viscoelasticity of surfactant monolayers. *J. Colloid Interface Sci.* 170, 358–366.
- Joly, M., 1972. Rheological properties of monomolecular films. Part II. Experimental results, theoretical interpretation, applications. In: Matijevic, E. (Ed.), *Surface and Colloid Science*, vol. 5. Wiley, New York, 79–194.
- Joos, P., Bleys, G., 1983. Desorption from slightly soluble monolayer. *Colloid Polym. Sci.* 261, 1038–1042.
- Kato, T., Iriyama, K., Araki, T., 1992. The time of observation of  $\pi$ -A isotherms. III. Studies on the morphology of arachidic acid monolayers, observed by transmission electron microscopy of replica samples of one-layer Langmuir–Blodgett films using plasma-polymerization. *Thin Solid Films* 210/211, 79–81.
- Kunieda, M., Nakaoka, K., Liang, Y., Miranda, C.R., Ueda, A., Takahashi, S., Okabe, H., Matsuoka, T., 2010. Self-accumulation of aromatics at the oil–water interface through weak hydrogen bonding. *J. Am. Chem. Soc.* 132, 18281–18286.
- Loglio, G., Tesei, U., Cini, R., 1984. Dilational properties of monolayers at the oil–water interface. *J. Colloid Interface Sci.* 100, 393–396.
- Lucassen, J., 1992. Dynamic dilational properties of composite surfaces. *Colloids Surf. A: Physicochem. Eng. Aspects* 65, 139–149.
- Mazurek, A.Z., Pogorzelski, S.J., Boniewicz-Szmyt, K., 2008. Evolution of natural sea surface film structure as a tool for organic matter dynamics tracing. *J. Mar. Syst.* 74, 52–64.
- Mohammed, R.A., Baily, A.I., Luckham, P.F., Taylor, S.E., 1993. Dewatering of crude oil emulsions. 2. Interfacial properties of the asphaltene constituents of crude oil. *Colloids Surf.* 80, 237–245.
- Nino, M.R.R., Wilde, P.J., Clark, D.C., Patino, J.M.R., 1998. Surface dilational properties of protein and lipid films at the air–water interface. *Langmuir* 14, 2160–2166.
- Nour, A.H., Suliman, A., Hadow, M.M., 2008. Stabilization mechanism of water-in-crude oil emulsions. *J. Appl. Sci.* 8, 1571–1575.
- Olanisebe, E.B., Isehunwa, S.O., 2013. Effect of pH on interfacial tension and crude oil–water emulsion resolution in the Niger delta. *J. Petrol. Gas Eng.* 4, 198–202.
- Pogorzelski, S.J., 1992. Isotherms of natural sea surface films: a novel device for sampling and properties studies. *Rev. Sci. Instrum.* 63, 3773–3776.
- Pogorzelski, S.J., 1996. Application of 2D polymer film scaling theory to natural sea surface films. *Colloids Surf. Physicochem. Eng. Aspects* 114, 297–309.
- Pogorzelski, S.J., Kogut, A.D., 2003. Structural and thermodynamic signatures of marine microlayer surfactant films. *J. Sea Res.* 49, 347–356.
- Pogorzelski, S.J., Kogut, A.D., Mazurek, A.Z., 2006. Surface rheology parameters of source-specific surfactant films as indicators of organic matter dynamics. *Hydrobiologia* 554, 67–81.
- Pogorzelski, S.J., Stortini, A.M., Loglio, G., 1994. Natural surface film studies in shallow coastal waters of the Baltic and Mediterranean Seas. *Cont. Shelf Res.* 14, 1621–1643.
- Ravera, F., Ferrari, M., Santini, E., Liggieri, L., 2005. Influence of surface processes on the dilational visco-elasticity of surfactant solutions. *Adv. Colloid Interface Sci.* 117, 75–100.
- Sharqawy, M.H., Lienhard, J.H., Zubair, S.M., 2010. Thermophysical properties of seawater: a review of existing correlations and data. *Desalin. Water Treat.* 16, 354–380.
- Takamura, K., Loahardjo, N., Winoto, W., Buckley, J., Morrow, N.R., Kunieda, M., Liang, Y., Matsuoka, T., 2012. Spreading and retrac-



- tion of spilled crude oil on sea water. In: Younes, M. (Ed.), *Crude Oil Exploration in the World*. In Tech, China, 107–124.
- Van Hunsel, J., Joos, P., 1989. Study of the dynamic interfacial tension at the oil/water interface. *Colloid Polym. Sci.* 267, 1026–1035.
- Van Vleet, E.S., Williams, P.M., 1983. Surface potential and film pressure measurements in seawater systems. *Limnol. Oceanogr.* 28, 401–414.
- Vargaftik, N.B., Volkov, B.N., Voljak, L.D., 1983. International tables of the surface tension of water. *J. Phys. Chem. Ref. Data* 12, 817–820.
- Yamabe, T., Moroi, Y., Abe, Y., Takahasi, T., 2000. Micelle formation and surface adsorption of N-(1,1-dihydroperfluoroalkyl)-N,N,N-trimethylammonium chloride. *Langmuir* 16, 9754–9758.
- Yarranton, H.W., Hussein, H., Masliyah, J.H., 2000. Water-in-hydrocarbon emulsions stabilized by asphaltenes at low concentrations. *J. Colloid Interface Sci.* 228, 52–63.